

# Constitutive modeling of the large strain behavior of crushable foams using the element-free Galerkin method

Guilherme da Costa Machado, Marcelo Krajnc Alves

*Dpto de Eng Mecânica - GMAC, UFSC, Florianópolis, SC – Brazil*

Hazin Ali Al-Qureshi

*Dpto de Eng. Mecânica - LabMat, UFSC, Florianópolis, SC – Brazil*

Rodrigo Rossi

*Dpto de Eng. Mecânica, UCS, Caxias do Sul, RS – Brazil*

## Abstract

This paper describes a constitutive law modeling isotropic polymeric foam materials. Focus has been placed on modeling the relative density dependency effect on polymeric foams subjected to large deformations using a volumetric hardening law. The model assumes the deformation measure to be given by the logarithmic, or Hencky, strain tensor with a conjugate stress measure, which is given by the rotated Kirchhoff stress. Numerical implementation scheme for the constitutive model is described and has been implemented using the element-free Galerkin method in a finite strain framework. The imposition of the essential boundary condition is made by the application of the Augmented Lagrangian method. Numerical examples are presented, under axisymmetric assumption, in order to attest the performance of the proposed numerical scheme.

Keywords: polymeric foams, large deformations, finite plasticity, element-free Galerkin

## 1 Introduction

The polymeric foams are more and more used in industry and in domestic applications. Made of a skeleton of more or less regular open or closed cells, here cells are the basic unit of these materials; they have a high energy absorption capacity, particularly useful for shock applications, acoustic and thermal insulating properties, and in some cases, for filtering applications. For these reasons, they are widely used in aircraft and automotive industry, buildings and packaging. Combining good mechanical properties with a low density, rigid polymer foams can also be used as structural materials. Whatever their use, their optimization needs the understanding of their microstructure/macroscopic mechanical

property relationships. Indeed, the mechanical response of these materials depends on their architecture, and on the intrinsic properties of the polymer in the cell wall. The architecture is determined by the cell wall thickness, the size distribution and the cells shape.

The literature presented many models to predict the behavior of these materials. Theoretical studies on foam have mainly addressed the behavior of low density foams. The structures of these foams are simulated by a compact assembly of walls and struts. All these models can be divided into two groups: complex modeling approaches based on finite element method which try to describe as finely as possible the foam microstructure; or simpler and more numerous models which largely simplify this microstructure such as [1]. These models are based on the assembly of geometric symmetric cells and relate analytically the elastic material properties and yield stress to the foam relative density. In the case of very high density foams, made of spherical cells that are closed and isolated ones from the others, the materials can be considered as porous.

The useful properties of cellular solids depend on the material from which they are made, their relative density, and their internal geometrical structure. It is important to link the physical properties of cellular solids to their density and complex microstructure, in order to understand how such properties can be optimized for a given application. Thus, for this class of material we will consider an elasto-plastic model, which incorporates, a hyperelastic constitutive relation that depends on the relative density of the material. This dependence inclusion can be justified by foam structures, which usually experience a large volumetric reduction in a usual compressive process, as show in [2]. On the other hand, the plastic phase is described by a modified  $J_2$  model, with a volumetric hardening law motivated by the experimental observation that shows a different response in compression and tension.

The adopted formulation considers: a *total Lagrangian* description of the finite deformation problem; a multiplicative decomposition of the deformation gradient, into a plastic and an elastic part; and a constitutive formulation, given in terms of the logarithmic deformation measure, or *Hencky* measure, and the rotated *Kirchhoff* stress. The use of the rotated Kirchhoff stress together with the logarithmic strain measure was first described in [3] and [4] and also studied by others authors, such as [5]. The advantage of choosing this conjugate stress-strain pair in the formulation of the constitutive relation is that it leads to a return mapping whose form is the same as the one derived in the small deformation plasticity framework.

## 2 Kinematics of deformation

The plasticity model presented in this paper considers the multiplicative decomposition of the deformation gradient  $\mathbf{F}$  into an elastic deformation,  $\mathbf{F}^e$ , and a plastic deformation,  $\mathbf{F}^p$ , as illustrated in Figure 1. Thus,

$$F = \mathbf{F}^e \mathbf{F}^p \text{ with } \mathbf{F} = \nabla_X \varphi(X, t) \quad (1)$$

Moreover, since  $\mathbf{F}^e = \mathbf{R}^e \mathbf{U}^e$ , one may define the deformation measure to be given by the logarithmic or *Hencky* strain tensor, given by  $\mathbf{E}^e = \ln(\mathbf{U}^e)$ .

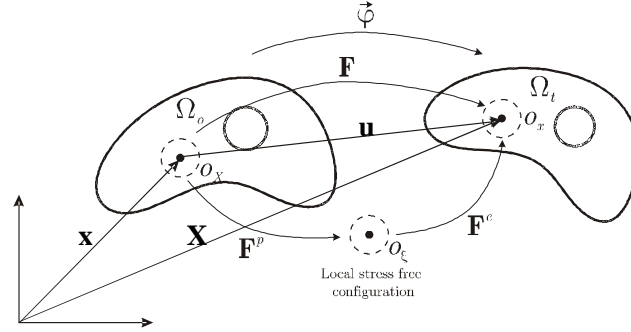


Figure 1: Multiplicative decomposition of the deformation gradient.

Hill [6] pointed out that the stress-strain pairs must be such that the rate of work density remains preserved. The enforcement of this criterion together with the assumption of an isotropic response of the material leads to the determination of the conjugate stress measure, which is given by the *rotated Kirchhoff* stress  $\bar{\tau}$ ,

$$\bar{\tau} = (\mathbf{R}^e)^T \tau (\mathbf{R}^e), \quad (2)$$

where  $\tau$  is the *Kirchhoff* stress,  $\tau = \det(F)\sigma$ , with  $\sigma$  denoting the *Cauchy* stress.

### 3 A brief description of the element-free Galerkin method

*Moving least square approximation:* The usage of the *Moving Least Square Approximation*, proposed by [7], enables the construction of an approximate function  $u^h(X)$  that fits a discrete set of data  $u_I = \{u_I, I=1, \dots, n\}$ , where:

$$u^h(X) = \sum_{I=1}^n \Phi_I(X) u_I \quad (3)$$

$$\Phi_I(X) = p(X) \cdot A(X)^{-1} b_I(X) \quad (4)$$

$$A(X) = \sum_{I=1}^n w(X - X_I) [p(X_I) \otimes p(X_I)] \quad (5)$$

$$b_I(X) = w(X - X_I) p(X_I) \quad (6)$$

in which:  $\{p_j(X), j = 1, \dots, m\}$  represents the set of intrinsic base functions;  $w(X - X_I)$  is a weight function centered at  $X_I$ ;  $\Phi_I(X)$  is the derived global shape function, defined at particle  $X_I$ ; and  $A(X)$  is the moment matrix.

*Element-free Galerkin weight functions:* One of the most used weight function is the quartic-spline function, which is given as:

$$w(r) = \begin{cases} 1 - 6r^2 + 8r^3 - 3r^4, & \text{for } r \leq 1.0 \\ 0, & \text{for } r > 1.0 \end{cases} \quad (7)$$

in which  $r = r_I/\bar{r}_I$  with  $r_I = \|X - X_I\|$ . The radius  $\bar{r}_I$ , defining the support of  $w(X - X_I)$ , is determined by

$$\bar{r}_I = s \cdot r_{I \max}, \quad s > 1, \quad s \in R \text{ with } r_{I \max} = \max_i \|X_i - X_I\|, \quad i \in J_I, \quad (8)$$

where  $J_I$  represents the set of adjacent nodes associated with  $X_I$ . An example of the covering of a given domain is illustrated in Figure 2.

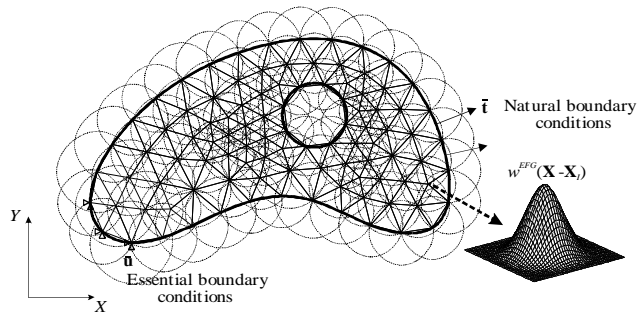


Figure 2: An example of body coverage by the EFG

#### 4 Constitutive modeling

In this section a rate-independent constitutive model is presented for isotropic polymeric foam material. A volumetric hardening model is motivated by the experimental observation that foam structures usually experience a different response in compression and tension. In compression the ability of the material to deform volumetrically is enhanced by cell wall buckling processes as described by [1]. It is assumed that the foam cell deformation is not recoverable instantaneously and can, thus, be idealized as being plastic for short duration events. In tension, on the other hand, cell walls break readily; and as a result the tensile load bearing capacity of crushable foams may be considerably smaller than its compressive load bearing capacity. The volumetric hardening model assumes the evolution of the yield surface is controlled by the volumetric plastic strain experienced by the material.

#### 4.1 Definition of the yield surface

In order to define the yield function, we must introduce some few definitions. The deviatoric rotated Kirchhoff stress, the effective rotated Kirchhoff stress, and the pressure stress, in that order, are given by

$$\bar{\tau}^D = \bar{\tau} - \frac{1}{3} \text{tr}(\bar{\tau}) I, \quad (9)$$

$$q = \sqrt{\frac{3}{2} \bar{\tau}^D : \bar{\tau}^D}, \quad (10)$$

$$p = -\frac{1}{3} \text{tr}(\bar{\tau}). \quad (11)$$

In this work we consider the yield function for crushable foam materials to be defined in terms of the Kirchhoff stress measure and given by

$$\mathcal{F}(q, p) = \sqrt{q^2 + \alpha^2 \left( p - \left[ \frac{p_c - p_t}{2} \right] \right)^2} - \alpha \left[ \frac{p_c + p_t}{2} \right] \leq 0, \quad (12)$$

in which  $\alpha = \alpha(\bar{\varepsilon}_k)$  and  $p_c = p_c(\bar{\varepsilon}_k)$  are a function of the internal variables  $\bar{\varepsilon}_k$ . The evolution of the yield ellipse is controlled by a plastic strain measure,  $\bar{\varepsilon}_1 \equiv \varepsilon_v^p$ , which is the volumetric compacting plastic strain, as shown in Figure 3, defined as

$$\varepsilon_v^p = -\ln(J^p) \text{ where } J^p = \det(F^p) \quad (13)$$

used in the volumetric hardening model, and the axial plastic strain,  $\bar{\varepsilon}_2 \equiv \varepsilon_a^p$ , whose definition, in a unilateral compression test, is given by

$$\varepsilon_a^p = -\ln\left(\frac{L^p}{L_o}\right), \quad (14)$$

where  $L^p$  is the unloaded length, after the deformation has been applied, and  $L_o$  is the length of the initial configuration of the reference specimen.

Here, we consider the hydrostatic tension strength,  $p_t$ , being related to the current compressive hydrostatic yield stress as  $p_t = \zeta p_c$ , where  $\zeta$  represents a constant of proportionality. Consequently, the expansion in the tensile  $p$ -direction is proportional to the hardening of the compressive  $p$ -direction. However, we assume the hydrostatic compression strength,  $p_c$ , to evolve as a result of compaction (increase in density) or dilation (reduction in density) of the material, i.e.

$$p_c = p_c(\varepsilon_v^p). \quad (15)$$

Moreover, the parameter  $\alpha$  is considered to depend on the volumetric compacting plastic strain  $\varepsilon_v^p$  and also on the axial plastic strain  $\varepsilon_a^p$ , i.e.,  $\alpha = \alpha(\varepsilon_v^p, \varepsilon_a^p)$ , given in a uniaxial state by

$$\alpha = \frac{\bar{\tau}_y}{\left\{ p_t p_c - \frac{1}{3} \bar{\tau}_y (p_t - p_c) - \frac{1}{9} \bar{\tau}_y^2 \right\}^{\frac{1}{2}}}. \quad (16)$$

Thus, the parameters  $p_c(\varepsilon_v^p)$  and  $\alpha(\varepsilon_v^p, \varepsilon_a^p)$  are sufficient to define the center and the lengths of the major and minor axes of the yield ellipse. These parameters are variables which are functions of the volumetric compacting plastic strain  $\varepsilon_v^p$ , which describes the so-called consolidation phenomenon, [8], and on the effective axial plastic strain  $\varepsilon_a^p$ . The two consolidation variables ( $\alpha, p_c$ ) are uniquely determined by the knowledge of two experimental tests, given by the uniaxial and hydrostatic compression tests. Thus,  $\mathcal{F} = \mathcal{F}(\alpha, p_c)$  where  $\alpha$  and  $p_c$  are material parameters.

#### 4.2 The non-associative plastic flow potential

The plastic modified strain rate for the non associative volumetric hardening model is assumed to be

$$\bar{D}^p = \dot{\lambda} \frac{\partial \mathcal{G}}{\partial \bar{\tau}}, \quad (17)$$

complemented by postulating a null plastic spin, compatible with plastic isotropy, i.e.,  $\bar{W}^p = 0$ . Here,  $\dot{\lambda}$  is the plastic multiplier which must satisfy the Kuhn-Tucker conditions:  $\mathcal{F} \leq 0$ ,  $\dot{\lambda} \geq 0$  and  $\dot{\lambda} \mathcal{F} = 0$ .

The evolution of the plastic deformation and the plastic flow potential, shown in Figure 3, are respectively

$$\dot{F}^p = \bar{D}^p F^p \quad (18)$$

$$\mathcal{G}(q, p) = \sqrt{q^2 + \beta^2 p^2}, \quad (19)$$

where  $\beta$  is related to the plastic Poisson's ratio  $\nu_p$  by

$$\beta = \frac{3}{\sqrt{2}} \sqrt{\frac{1 - 2\nu_p}{1 + \nu_p}}. \quad (20)$$

The plastic Poisson's ratio, which is the ratio of the transverse to the longitudinal plastic strain under uniaxial compression, should be defined, and it must be in the range of -1 and 0.5, i.e.,  $\nu_p \in [-1, 0.5]$ . The upper limit,  $\nu_p = 0.5$ , corresponds to an incompressible plastic flow. The usual assumption, for polymeric foams is to consider  $\nu_p = 0.0$ . In the absence of the knowledge of the plastic Poisson's ratio, the consideration of a zero plastic Poisson's ratio is a reasonable assumption, as shown in [8], [1] and [9].

#### 4.3 Hyperelastic response

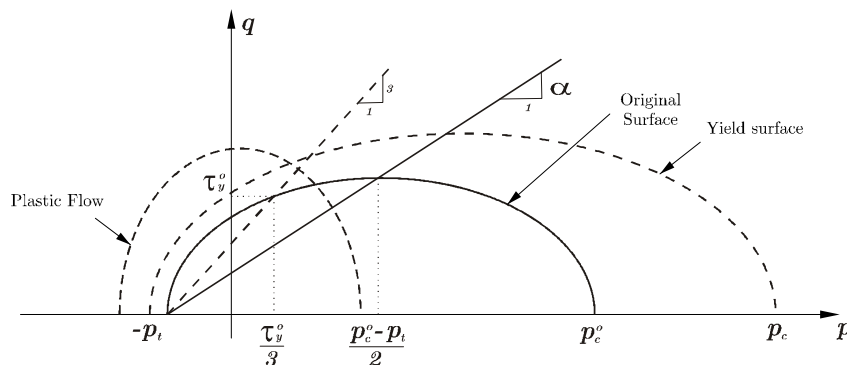
Based on the hypothesis of multiplicative split of the deformation gradient and the deformation measure to be given by the logarithmic or *Hencky* strain tensor we may write the hyperelastic law as

$$\bar{\tau} = D(\rho^*) E^e \quad (21)$$

where

$$D(\rho^*) = 2\mu(\rho^*) I + \left( K(\rho^*) - \frac{2}{3}\mu(\rho^*) \right) (I \otimes I) \quad (22)$$

in which  $D(\rho^*)$  is the fourth order elasticity tensor,  $I$  is the fourth order identity tensor,  $I$  is the second order identity tensor,  $K(\rho^*)$  is the bulk modulus and  $\mu(\rho^*)$  is the Lamé's coefficient or the shear modulus.


 Figure 3: Yield surface and flow potential on  $p - q$  stress space.

The above constitutive equation include the effect of the relative density,  $\rho^*$ , which is defined by the ratio of the foam density,  $\rho$ , by the fully compact material density,  $\rho_M$ . Thus,

$$\rho^* = \frac{\rho}{\rho_M}. \quad (23)$$

At this point, writing the continuity equation with relation of relative density we obtain

$$\rho_o^* = \det [F] \rho^*, \quad (24)$$

in which  $\rho_o^* = \rho_o^*(X)$  denotes the initial relative density, defined in the reference configuration, and  $\rho^* = \rho^*(X, t)$  the actual relative density, defined at the reference configuration.

The model considers

$$\nu(\rho^*) = \nu_o = \text{constant term} \quad (25)$$

and

$$E(\rho^*) = (\rho^*)^\gamma E_M \quad (26)$$

with  $\nu_M$  representing the Poisson's ratio and  $E_M$  the Young's modulus of the fully dense material. Thus,  $\nu_o$ ,  $E_M$  and  $\gamma$  must be identified by experimental tests.

The hypothesis of considering  $\nu(\rho^*)$  being independent of the relative density is observed experimentally, i.e., is a reasonable assumption. Thus, the strong dependency is through the Young's modulus.

#### 4.4 Hardening rules

The scalar valued functions  $H_a(\varepsilon_a^p)$  and  $H_p(\varepsilon_v^p)$  are the hardening functions determined in a uniaxial and hydrostatic compressive tests respectively.

$$\bar{\tau}_y = \bar{\tau}_y^o + H_a(\varepsilon_a^p) \quad (27)$$

$$p_c = p_c^o + H_p(\varepsilon_v^p) \quad (28)$$

where,  $p_c^o$  is the initial yield compression stress obtained in a hydrostatic test and  $\bar{\tau}_y^o$  is the initial yield stress obtained in a uniaxial compression test.

Notice that, in a non uniaxial loading case we are not able to identify  $\bar{\varepsilon}_a^p$ . Thus, the axial plastic strain measure must be modified in terms of a new plastic measure that is computable in a general loading case. Now, in a uniaxial compression test we have

$$\varepsilon_a^p = \frac{\varepsilon_v^p}{(1 - 2\nu_p)} \quad (29)$$

which allow us to replace  $\varepsilon_a^p$  by the measure  $\varepsilon_v^p$  in the hardening rule.

## 5 Total Lagrangean formulation

### 5.1 Strong formulation

The finite deformation elasto-plastic problem may be stated as: Determine  $\mathbf{u}$  such that

$$\begin{aligned} \operatorname{div} P + \rho_o \bar{b} &= 0 \quad \text{in } \Omega_o \\ \mathbf{P}m &= \bar{t} \quad \text{on } \Gamma_o^t \\ u &= \bar{u} \quad \text{on } \Gamma_o^u \end{aligned} \quad (30)$$

where  $\mathbf{P}$  is the first *Piola-Kirchoff* stress,  $\mathbf{m}$  is the outer normal to  $\partial\Omega_o$  and  $\bar{b}$ ,  $\bar{t}$  and  $\bar{u}$  are the prescribed body force, traction vector and displacement field respectively.

### 5.2 Incremental weak form of the problem

Let  $\mathcal{K} = \{u \mid u_i \in W_p^1(\Omega), u = \bar{u} \text{ em } \Gamma_o^u\}$  denote the set of admissible displacements and  $\mathcal{V} = \{\delta u \mid \delta u_i \in W_p^2\}$  the set of admissible variations. The weak formulation of the problem may be stated as: Find  $u_{n+1} \in \mathcal{K}$  such that  $F(u_{n+1}; \delta u) = 0 \quad \forall \delta u \in \mathcal{V}$ , i.e.,

$$F(u_{n+1}^k; \delta u) = \int_{\Omega_o} P(u_{n+1}^k) \cdot \nabla_{\bar{X}} \delta u^h d\Omega_o - \int_{\Omega_o} \rho_o \bar{b}_{n+1} \cdot \delta u^h d\Omega_o + \int_{\Gamma_o^t} \bar{t}_{n+1} \cdot \delta u^h dA_o + F^u(u_{n+1}^k, \delta u) \quad (31)$$

The imposition of the essential boundary condition is done by the application of the Augmented Lagrangian method, where the term associated with the imposition of the essential boundary conditions is given by

$$F^u(u_{n+1}^k, \delta u) = - \int_{\Gamma_o^u} q^u(u_{n+1}^k, \varepsilon_u, \lambda_{u_{n+1}}^k) \cdot \delta u d\Gamma_o^u \quad (32)$$

where  $q^u$  is given by

$$q^u(u_{n+1}^k, \varepsilon_u, \lambda_{u_{n+1}}^k) = - \left[ \lambda_{u_{n+1}}^k + \frac{1}{\varepsilon_u} (u_{n+1}^k - \bar{u}_{n+1}) \right] \quad (33)$$

The Lagrange multipliers are updated as

$$\lambda_{u_{n+1}}^{k+1} = - \left[ \lambda_{u_{n+1}}^k + \frac{1}{\varepsilon_u} (u_{n+1}^k - \bar{u}_{n+1}) \right] \quad (34)$$

which shows that the lagrangian multiplier represents physically the traction acting at the essential boundary condition due to the reaction force.

## 6 Numerical results

### 6.1 Uniaxial compression test

Here, the simulation of a uniaxial compression test is presented and confronted with de experimental data obtained in [8]. The specimen has an initial area of  $2500\text{mm}^2$  and  $50\text{mm}$  of height. The material parameters used in this analysis are described in 6.2. The process consists in prescribing the displacement of the upper part of the specimen, with a total upsetting of  $u_y = 30\text{mm}$ , applied in order to compress the body. Due to the axisymmetry condition, only half of the domain is modeled. This example uses an integration mesh with 4 triangular cells and 9 EFG particles. A support of influence of  $s=1.5$  together with a 7 points integration *Gauss-Legendre* scheme is employed in the analysis. In addition, an external penalty parameter of  $\varepsilon_u=10^{-6}$ . is used in the analysis.

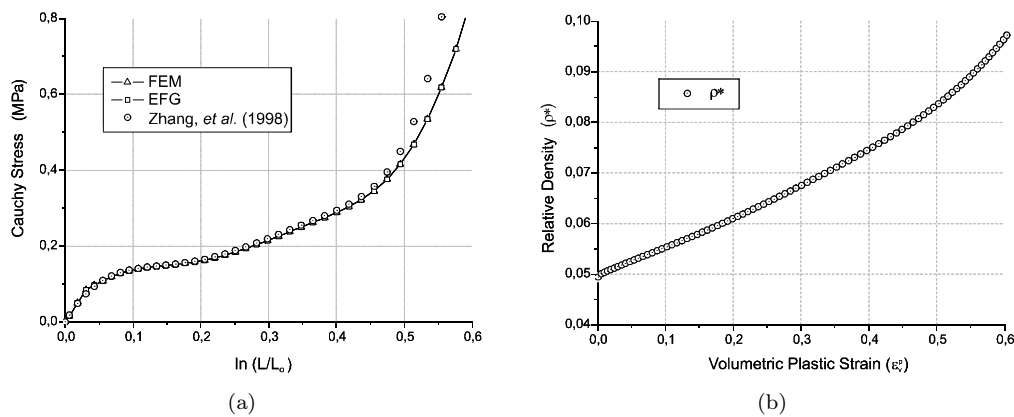


Figure 4: Uniaxial simulation: (a) Cauchy Stress versus the logarithm strain; (b) Variation of relative density with respect the volumetric plastic strain.

## 6.2 Conical slab

This example considers an axisymmetric problem that consists in the upsetting of a conical slab, whose dimensions are:  $r_1=90mm$ ;  $r_2=45mm$ ;  $h=100mm$ . The analysis consists in prescribing the displacement of the upper wall, with a total upsetting of  $u_y=80mm$ , which was applied in 1000 step-loads, in an integration mesh with 240 cells and 143 EFG particles. The parameters used in this analysis are the same:  $\tau_y^o = 82,034$  KPa,  $E_m = 928,092$  MPa,  $\nu = 0,25$ ,  $p_c^o = 40,470$  KPa,  $\rho_o^* = 0,049$ ,  $\gamma = 1,54$ ,  $\zeta = 0,30$ ,  $\nu_p = 0,00$  and  $c = 0,30$ . Again, 7 points integration *Gauss-Legendre* scheme is used, as well the support of influence  $s=1.5$  and the penalty parameter  $\varepsilon_{\cdot u}=10^{-6}$ .

Table 1: Material parameters.

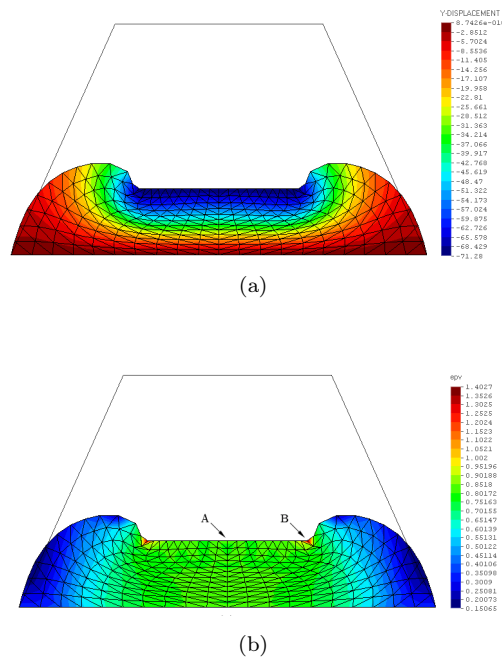


Figure 5: Fringes results from: (a) displacement on  $y$  direction,  $u_y$ ; (b) volumetric plastic strain,  $\varepsilon_v^p$ .

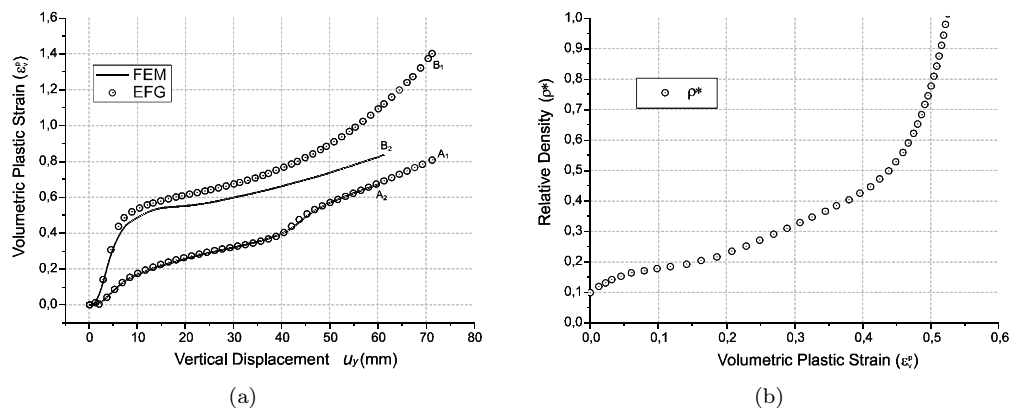


Figure 6: Uniaxial simulation: (a) Cauchy Stress versus the logarithm strain. The indexes A and B refers to the points indicated in Figure 5 and the sub indexes 1 and 2 refers to FEM and EFG methods respectively; (b) Variation of relative density with respect the volumetric plastic strain.

## 7 Discussion and conclusion

Polymeric foam constitutive behavior is extremely complex on the microstructural scale. Cellular buckling under compression initiates a long stress plateau. Further compression causes stress bottom up due to foam consolidation.

A rate-independent elasto-plastic foam constitutive model, that features a single-surface yield criterion, has been developed. A non associated plastic flow law and the relative density dependence showed reasonably prediction for the responses of rigid polymeric foams under the monotonic loading conditions.

One of the most relevant advantages in use the element-free Galerkin method, compared with the FEM, is the ability of the method to withstand the analysis of very large deformation processes, doing no remeshing, without breaking up. In addition, EFG method showed to be more robust to capture high deformation and deformation gradients, in which the material is subjected to a huge densification process, as shown in curves  $B1$  and  $B2$  in Figure 6, where the FE solution breaks up before the EFG solution.

The proposed polymeric foam model was tested with a typical foam problem and has performed adequately. From the above considerations, one may conclude that the proposed model and numerical procedure showed to be adequate for the simulation of large strain behavior of polymeric crushable foams under monotonic loading conditions.

## References

- [1] Gibson, L.J. & Ashby, M.F., *Cellular Solids: Structure and Properties*. 2nd, Cambridge University Press, 1997.
- [2] Roberts, A.P. & Garboczi, E.J., *Elastic moduli of model random three-dimensional closed-cell cellular solid*, volume 49 of *189-197*. Acta Materialia, 2001.
- [3] Eterovic, A.L. & Bathe, K.J., A hyperelastic-based large strain elasto-plastic constitutive formulation with combined isotropic-kinematic hardening using the logarithmic stress and strain measures. *International Journal for Numerical Methods in Engineering*, **30**, pp. 1099–1114, 1990.
- [4] Weber, G. & Anand, L., Finite deformation constitutive equations and a time integration procedure for isotropic, hyperelastic-viscoplastic solids. *Computer Methods in Applied Mechanics and Engineering*, **79**, pp. 173–202, 1990.
- [5] Akkaram, S. & Zabaraz, N., An updated lagrangian finite element sensitivity analysis of large deformations using quadrilateral elements. *International Journal for Numerical Methods in Engineering*, **52**, pp. 1131–1163.
- [6] Hill, R., Aspects of invariance in solid mechanics. *Advances in Applied Mechanics*, **18**, pp. 1–75, 1978.
- [7] Lancaster, P. & Salkauskas, K., Surfaces generated by moving least squares methods. *Mathematical of Computational*, **37**, pp. 141–158, 1981.
- [8] Zhang, J., Kikuchi, N., Yee, A. & Nusholtz, G., Constitutive modeling of polymeric foam material subject to dynamic crash loading. *International Journal of Impact Engineering*, **21(5)**, p. 369, 1998.
- [9] Gilchrist, A. & Mills, N.J., Impact deformation of rigid polymeric foams: experiments and fea modeling. *International Journal of Impact Engineering*, **25**, pp. 767–786, 2001.